# 22 Analysis of the effect of residual gas on HCCI combustion spatial structures using chemiluminescence measurements with a 4-stroke optical accessible engine and Rapid Compression Machine

(1) Satoshi KETADANI, (2) Kengo KUMANO, (3) Norimasa IIDA

(1)(2)(3) Keio University

3-14-1, Hiyoshi, Kouhoku-ku, Yokohama, Kanagawa, Japan

In the combustion chamber of the Homogeneous Charge Compression Ignition (HCCI) engine, inhomogeneity of fuel concentration, gas temperature, and gas composition exist that are produced by inlet condition, residual gas, flow, and heat transfer through the wall. HCCI combustion depends on the chemical reaction of fuel and oxygen. Therefore HCCI combustion is affected by these inhomogeneity. In this study, the effect of residual gas that generates inhomogeneity of gas temperature and gas composition in the combustion chamber on HCCI combustion was investigated with a 4stroke-engine and Rapid Compression Machine. The sample fuel was Di-methyl ether (DME). As a result, under the condition in which exists residual gas, chemiluminescence intensity was distributed more than under the condition of nonexistence of residual gas.

**Keywords**: *Engine combustion, Thermal Engineering, Fuel, HCCI Combustion , DME, Residual gas, inhomogeneity*

## 1. INTRODUCTION

Homogeneous charge compression ignition combustion (HCCI combustion) is taken into notice as the combustion system that can actualize high-efficiency and low-emission. The process of HCCI combustion depends on the chemical reaction of fuel and oxygen. For this reason, the control of ignition timing and combustion duration is difficult. Therefore, this impedes the realization of the HCCI engine. In order to solve these problems, calculations and experimentations regarding the control of HCCI combustion using inhomogeneity in premixed gas have been studied. There are inhomogeneity of fuel concentration, gas temperature, and composition. Research has been done on the inhomogeneity of in-cylinder gas temperature. Using multi-zone model calculations, it was reported that temperature stratification in the premixed gas before compression start affected the rate of pressure increase[1]. Research has been done on the inhomogeneity of fuel concentration and composition. In the calculations, using three dimensional chemical calculation with CFD, it was reported that the inhomogeneity of fuel concentration in the combustion chamber or mixed state of fresh gas and residual gas affected heat release and combustion duration[2][3]. In the experiment, the effect of inhomogeneity in fuel concentration in the premixed gas on HCCI combustion was studied using a 4-stroke optical accessible engine[4]. Additionally, it was reported that the inhomogeneity of fuel concentration affected heat release and combustion duration. In addition under the condition of inhomogeneous fuel concentration, flame structure was investigated. It was revealed that the flame under the inhomogeneous condition dispersed more spatially and temporarily than under the homogeneous condition. However, it is thought that this result includes some effects of residual gas. Residual gas generates inhomogeneity of gas temperature and composition. Therefore, in this study the effect of residual gas on HCCI combustion is investigated from flame structure analyzing chemiluminescence intensity using two dimensional luminescence measurements with a 4-stroke optical accessible engine and a rapid compression machine. The test fuel is Di-methyl ether (DME).

## 2. TEST FUELS

In this study, Di-methyl ether, (DME) which is an ether series fuel, is selected. Figure 1 and table 1 show the molecular structure and characteristics. DME/Air HCCI combustion has a clear low temperature reaction (LTR) and high temperature reaction (HTR). It was also reported that the

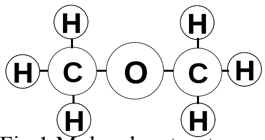

Fig.1 Molecular structure

Table1 Molecular property

| | |
|---|---|
| Chemical formula | $(CH_3)_2O$ |
| Molar weight(kg/mol) | 46.069 |
| Cetane Number | 55～60 |
| Lower Calorific Value(MJ/kg) | 28.8 |
| Specific heat(kJ/kg・K) | 2.99 |

chemiluminescence from CO+O+M=CO2+M accounted for the major part of the chemiluminescence of HTR[5][6].

### 3. The condition of nonexistence of residual gas

#### 3.1 Experimental setup

The Rapid compression machine (RCM) is selected as the engine to form the condition of nonexistence of residual gas. The experimental system chart and elements are shown in figure 2. The bore and stroke is 145 x 692mm, and the compression ratio $\varepsilon$ is 14.6. The moisture in the air is removed by silica gel. Next, the air is premixed with DME, and heated to 353K. The heated premixed gas flows into the cylinder. The intake pipe and wall surfaces of the cylinder are also heated to 353K. The measurement system chart is shown in figure 3. In-cylinder pressure is measured at the wall surface of the combustion chamber using non water cooling pressure pickup. In-cylinder gas temperature before compression start $T_s$ is mesured at the position located at 83mm from the wall surface. Chemiluminescence runs through two reflectors after running through two pices of quarz glass placed on the cylinder head, and the light having awavelength between 200 and 900nm is photographed by a framing camera. In other words, three-dimensional data is captured as two dimensional data. One pixel corresponds to a 0.67mm-squre.

#### 3.2 Analysis method

Figure 4 shows the definitions of the appearance time, and the disappearance time of LTR and HTR. In the logP-logV graph, the points that lose linearity are defined as the start of LTR and HTR. Ignition timing is evaluated from these *P* and *V*. Before ignition, in-cylinder gas temperature $T_c$ is calculated from equation (a) assuming adiabatic compression, because ignition occurs around the center of the combustion chamber, which is not influenced by the heat loss through the cylinder wall. After ignition, $T_c$ is calculated from the ideal gas equation (b). Adiabatic change is not approved because of heat release.

$$T_c(t_i) = \left(\frac{P(t_i-1)}{P(t_i)}\right)^{\frac{1}{\kappa(t_i-1)}} T(t_i-1) \quad \text{….(a)}$$

$$T_c(t_i) = \frac{P(t_i)\cdot V(t_i)\cdot n(t_{i-1})\cdot T(t_{i-1})}{P(t_{i-1})\cdot V(t_{i-1})\cdot n(t_i)} \quad \text{….(b)}$$

$T_c$: in-cylinder gas temperature [K], $t$: time [ms] $P$: in-cylinder gas pressure [Pa], $\kappa$: specific heat ratio, $n$: number of moles [mol], $V$: volume [m$^3$]

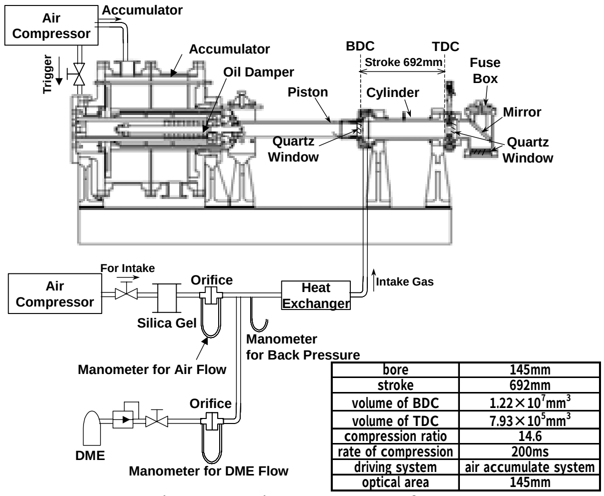


| | |
|---|---|
| bore | 145mm |
| stroke | 692mm |
| volume of BDC | 1.22×10$^7$mm$^3$ |
| volume of TDC | 7.93×10$^5$mm$^3$ |
| compression ratio | 14.6 |
| rate of compression | 200ms |
| driving system | air accumulate system |
| optical area | 145mm |

Fig.2 Experiment system of RCM

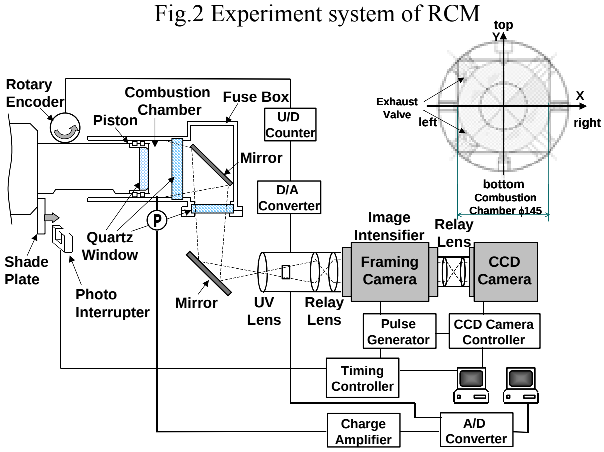

Fig.3 Measurement system of RCM

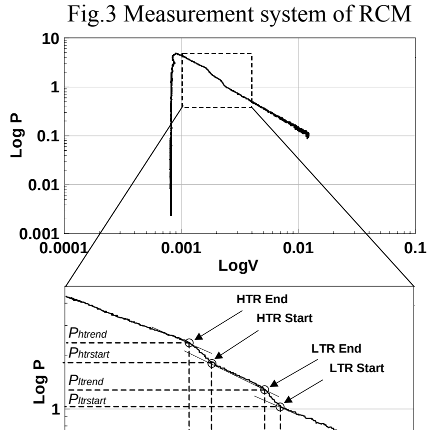

Fig.4 Definition of ignition timing

#### 3.3 Experimental results

(1) **Composition and temperature of in-cylinder gas before compression start** Figure 5 shows the mass ratio of in-cylinder gas composition. Under the condition of nonexistence of residual gas at 353K, fresh gas accounts for 100% of the in-cylinder gas and temperature.

(2) **Combustion characteristics** Figure 6 shows the histories of in-cylinder volume *V*, in-cylinder pressure *P*, and in-cylinder

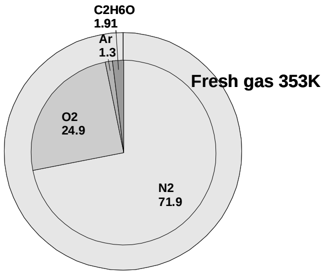


Fig.5 In-cylinder gas composition before compression start

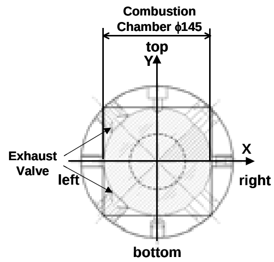


Fig.8 Definition of the X axis and Y axis

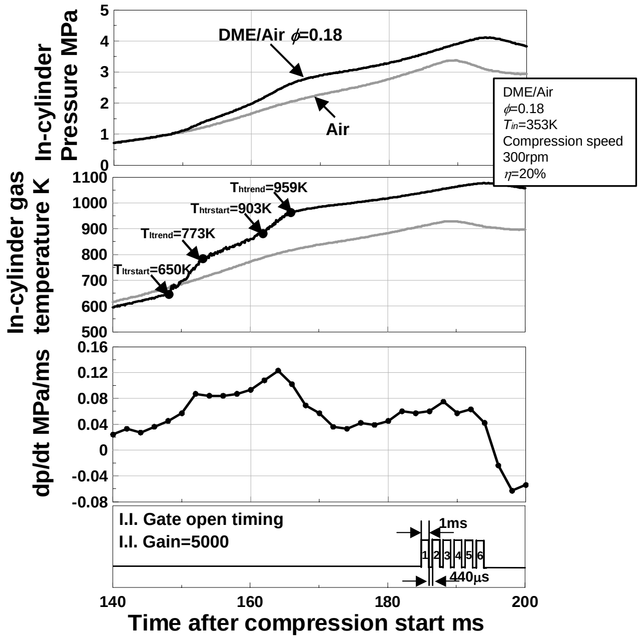


Fig.6 Histories of in-cylinder gas pressure, temperature, rate of pressure rize, and shooting timing

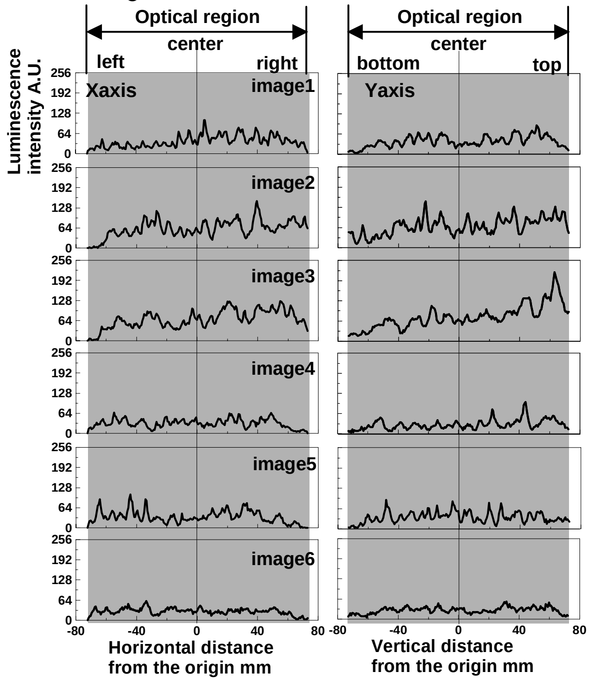


Fig.9 Histories of cheimiluminescence intensity on X axis and Y axis

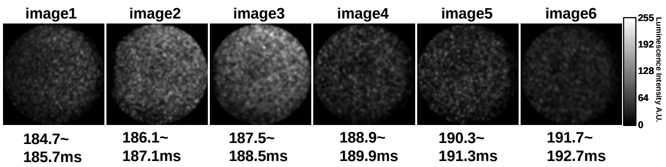


Fig.7 Two dimensional images

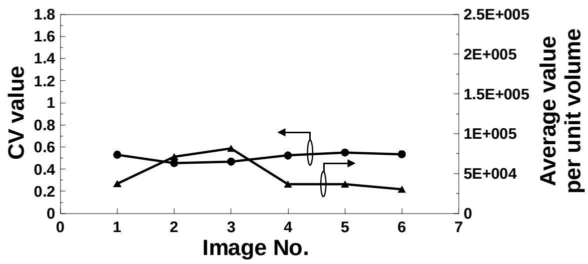


Fig.10History of CV value and average value

gas temperature $T_c$ at the compression speed approximately 300rpm, equivalence ratio of $\phi$=0.18, initial temperature of $T_{in}$=353K. LTR and HTR are observed in the historeis of $P$ and $T_c$. LTR temperature $T_{ltrstart}$ is 650K, and LTR duration $\Delta t_{ltr}$ is 3.2ms. HTR temperature $T_{htrstart}$ is 903K, and HTR duration $\Delta t_{htr}$ is 3.2ms. The maximum in-cylinder gas temperature $T_{max}$ is approximately 1076K. The combustion efficiency $\eta$ is 20%.

(3) **Two dimensional images** The target timing is HTR at exposure time $t_{ex}$=1ms, shoot duration $t_{sh}$=440µs, I,I,gain=5000. The in-cylinder gas temperature at shooting timing is from 1037K to 1073K. Figure 7 shows two dimensional images. Chemiluminescence is observed in the entire area of the combustion chamber from image1 to image6. The chemiluminscence intensity becomes stronger from image1 to image3. After this, chemiluminescence intensity becomes weaker from image4 to image6. Next, in figure 8, center of the combustion chamber is defined as original, and X axis and Y axis are defined. Figure 9 shows the histories of chemiluminescence intensity on the X and Y axes. Chemiluminescence occurs on all points of the X and Y axes. Figure 10 shows the history of average value per unit volume $I_{ave}$ and the CV value (= standard deviation A.U./average value A.U.). As has been previously described, two dimensional images are an integration of three dimensional data. Therefore, the difference in bore and stroke affect two dimensional images. In this paper, in order to eliminate the effect of the difference in bore and stroke, average chemiluminescence intensity per unit volume $I_{ave}$, which is determined by dividing the chemiluinescence intensity of the images obtained by the in-cylinder volume during shooting timing is used. The CV value is as index of distribution of chemiluminescence intensity

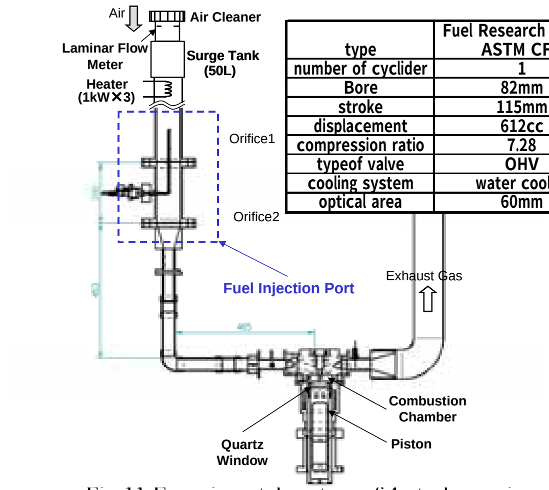


| type | Fuel Research Eingine ASTM CFR |
|---|---|
| number of cyclider | 1 |
| Bore | 82mm |
| stroke | 115mm |
| displacement | 612cc |
| compression ratio | 7.28 |
| typeof valve | OHV |
| cooling system | water cooled |
| optical area | 60mm |

Fig.11 Experimental system of 4-stroke engine

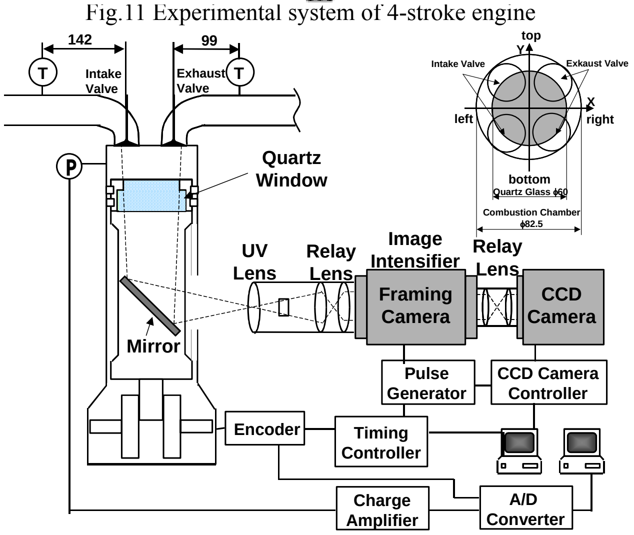


Fig.12 Measurement system of 4-stroke engine

without spatial factors. The smaller the CV value, the more uniform the chemiluminescence intensity in the combustion chamber. $I_{ave}$ becomes stronger from Image1 to Image3, and becomes weaker from Image3 to Image6. However, the CV value is approximately 0.5 in all images.

## 4. The condition of existence of residual gas

### 4.1 Experimental setup

The 4-stroke optical accessible engine is selected as the engine to form the condition of the existence of residual gas. Figure 11 and 12 show the experimental system chart and the elements. The bore and stroke is 82.5 x 115mm, and compression ratio $\varepsilon$ is 7.2. The air measured by a laminar flow meter is heated by a heater (1 kW x 3) located at 1400mm upstream from the intake valve. DME is injected from a port located 1100mm upstream from the intake valve. The injection nozzle is 115mm long and has 100 holes which have a diameter of 1.5mm each. Upstream from the fuel injection point, orifice plate 1 (ϕ35 x 1 hole) is provided for large scale mixing. Downstream from orifice plate 1, orifice plate 2 (ϕ5 x 19 holes) is provided for small scale mixing. In-cylinder pressure is measured by a cooled piezo

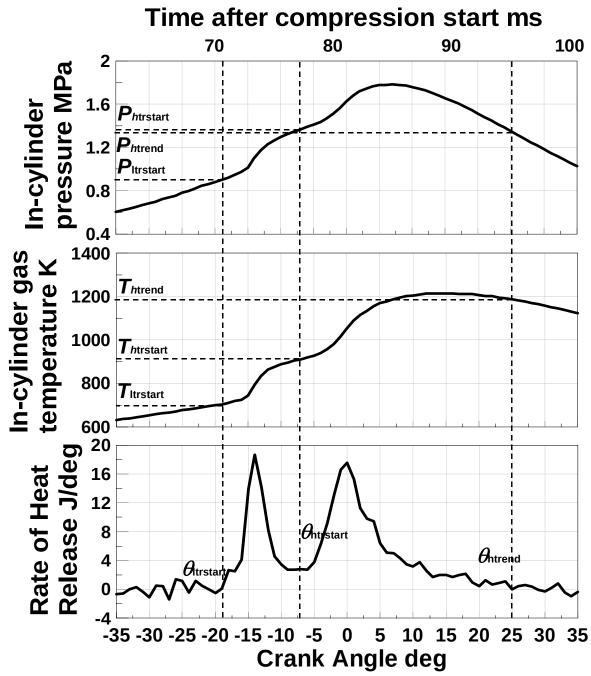


Fig.13 Definition of ignition timing

type pressure pick-up at the wall of the combustion chamber. Intake gas temperature $T_{in}$ is measured by a K type thermocouple located 142mm upstream from the intake valve. Exhaust gas temperature $T_{ex}$ is measured by a K type thermocouple located 99mm downstream from the exhaust valve. The optical area is ϕ60 in figure 12 Chemiluminescence runs through a reflector after running through one pices of quarz glass placed on the cylinder head, and the light having awavelength between 200 and 900nm is photographed by a framing camera. In other words, three-dimensional data is captured as two dimensional data. One pixel corresponds to a 0.27mm-squre.

### 4.2 Analysis method

Figure 13 shows the definitions of the appearance time, peak time, and disappearance time of LTR and HTR. The LTR appearance time is defined as the time when R.H.R. rises for the first time and the HTR disappearance time is defined as the time when R.H.R drops to zero level for the first time after the LTR appearance time. The LTR disappearance time and HTR appearance time are defined as the time when R.H.R. is minimal between the LTR and HTR peak times. In-cylinder gas temperature before compression start $T_s$ is calculated by enthalpy balance equation(c) assuming that mixing between fresh gas and residual gas occurs at the instant of intake valve closure. Before ignition, $T$ is calculated from the equation (d) assuming adiabatic compression. After ignition, in-cylinder gas temperature is calculated from the ideal gas equation (e).

$$T_s = \frac{m_f c_{p\_f} T_f + m_r c_{p\_r} T_r}{m_f c_{p\_f} + m_r c_{p\_r}} \quad \ldots\text{(c)}$$

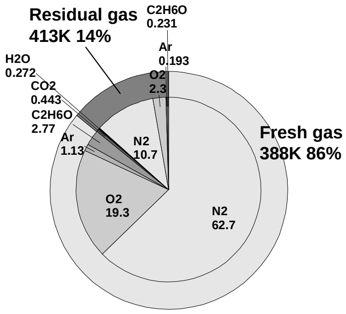


Fig.14 In-cylinder gas composition before compression start

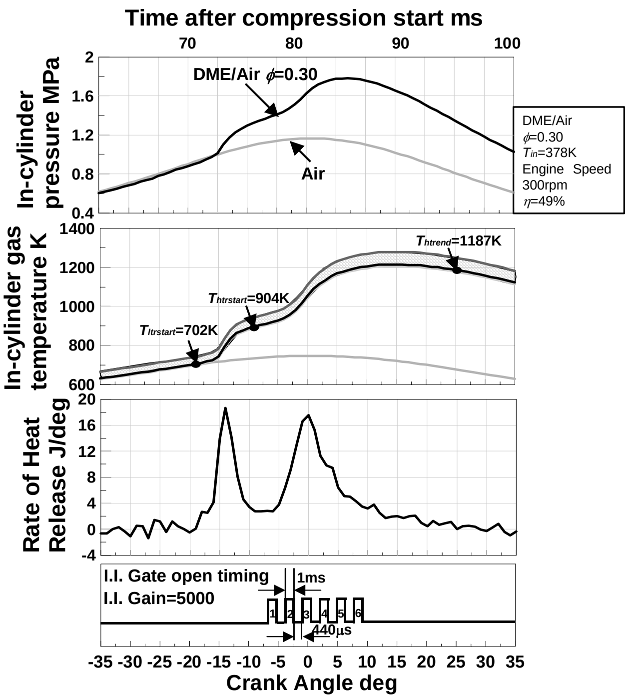


Fig.15 Histories of in-cylinder gas pressure, temperature, R.H.R, and shooting timing

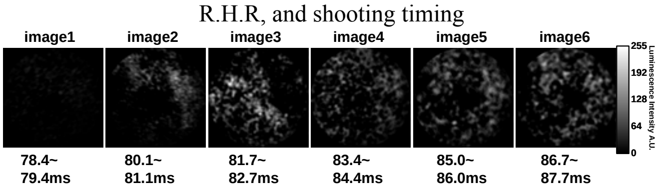


Fig.16 Two dimensional images

$$T_c(\theta_i)=\left(\frac{P(\theta_i-1)}{P(\theta_i)}\right)^{\frac{1}{\kappa(\theta_i-1)}}T(\theta_i-1)\quad\text{….(d)}$$

$$T_c(\theta_i)=\frac{P(\theta_i)\cdot V(\theta_i)\cdot n(\theta_{i-1})\cdot T(\theta_{i-1})}{P(\theta_{i-1})\cdot V(\theta_{i-1})\cdot n(\theta_i)}\quad\text{….(e)}$$

$T$: in-cylinder gas temperature [K], $Ts$: in-cylinder gas temperature before compression start [K] $\theta$: crank angle [degree] $P$: in-cylinder gas pressure [Pa], $\kappa$: specific heat ratio, $n$: number of moles [mol], $V$: volume [m$^3$], $c_p$: specific heat at constant pressure [kJ/kg/K], $m$: mass of gas[kg]

**4.3 Experimental results**

(1) **Composition and temperature of in-cylinder gas before compression start** Figure 14 shows the temperature of the in-cylinder gas and the mass ratio of its composition. The

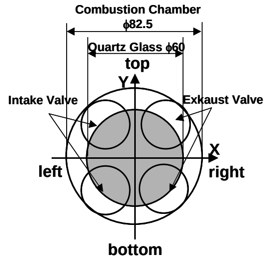


Fig.17 Definition of the X axis and Y axis

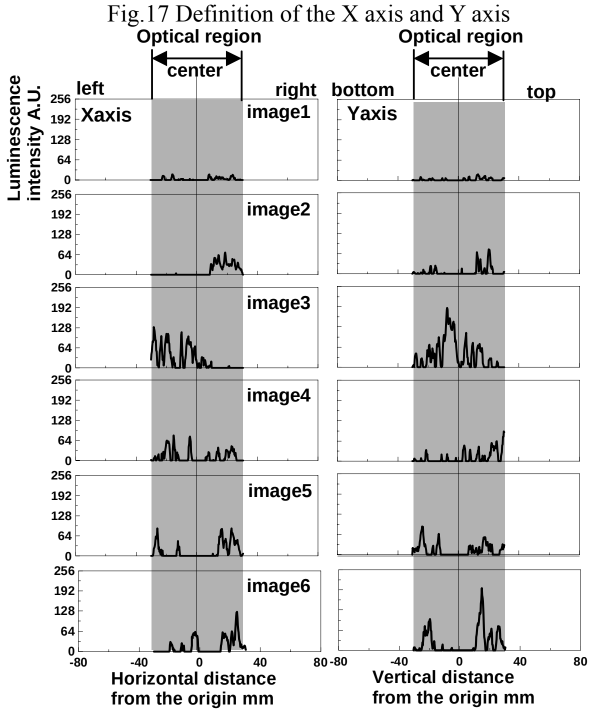


Fig.18 Histories of cheimiluminescence intensity on X axis and Y axis

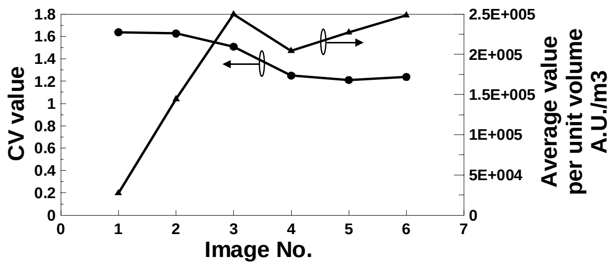


Fig.19 History of CV value and average value

volume of residual gas is defined as the difference between the volume of the combustion chamber when it is closed system and the inlet flow for one cycle. $T_r$ is defined as $T_{ex}$. The mass ratio of the gas composition of the residual gas is calculated by using amounts of DME, H2O, and CO2 evaluated by $\eta$. The maximum in-cylinder gas temperature before compression start $T_{s\_max}$ is defined as $T_r$=413K assuming that exhaust gas is not cooled off in the intake manihold and stays in the comubustion chamber. The minimum in-cylinder gas temperature before compression start $T_{s\_min}$ is defined as $T_{in}$=388K. The actual in-cylinder gas temperature before compresssion start is thought to disperse from $T_{s\_min}$ to $T_{s\_max}$. The average in-cylinder gas temperature $T_s$ is 391K according to equation(c).

(2) **Combustion characteristics** Figure 15 shows the

histories per 1 cycle of $P$, $T$, and the rate of heat release $R.H.R$ at engine speed $Ne$=300rpm, $\phi$=0.30, $T_{in}$=388K. $\Delta t_{ltr}$ is 5.6ms and $\Delta t_{htr}$ is 15ms. Using $T_{s\_min}$, $T_{ltrstart}$ is 703K and $T_{htrstart}$ is 904K. When $T_{s\_max}$ is used, $T_{ltr}$ is 745K and $T_{hrt}$ is 959K. When $T_s$ is used, $T_{ltr}$ is 702K and $T_{htr}$ is 904K. The actual $T$ stays within the shaded area in figure16. $T_{max}$ stays between 1206K and 1279K.

(3) **Two dimensional images** The target timing is HTR at $t_{ex}$=1ms, $t_{sh}$=668μs, I.I.gain=5000. The in-cylinder gas temperature at shooting timing is from 926K to 1214K. Figure16 shows two dimensional images. Chemiluminescence is observed from image2 to image6. Under the condition of nonexistence of residual gas, cheimiluminescence is not observed in the entire area of the combustion chamber. Next, in figure 17, the X axis and Y axis are defined as in figure 8. Figure 18 shows the histories of chemiluminescence intensity on the X and Y axes. The area where the chemiluminescence intensity is 0 is more distinct than under the condition of nonexistence of residual gas. Figure 19 shows the history of $I_{ave}$ and CV value. $I_{ave}$ becomes larger from image1 to image6. The CV value becomes smaller from image1 to image6. The CV value is over 1.2 in all images. The CV value under the condition of existence of residual gas is constantly larger than under the condition of nonexistence of residual gas.

## 5. Discussion

In-cylinder pressure is limited within 5MPa for the safe operation of the RCM. In the results, $\phi$ is limited and $\eta$ is low. The experiment with the 4-stroke optical accessible engine is at low $\eta$. Under the condition of nonexistence of residual gas, chemiluminscence is observed in the entire area of the combustion chamber. However, under the condition of existence of residual gas, chemiluminescence is not observed in the entire area of the combustion chamber in all of the images. Figure9 and 18 showed the history of chemiluminescence intensity on the X axis and Y axis. The RCM used in this study had gas temperature stratification from top to bottom on the Y axis. However, RCM had no temperature stratification on Xaxis. On the other hand, distribution of in-cylinder gas temperature and composition in the 4-stroke engine has not been investigated. Comparing the two conditions on the X axis, even though $I_{ave}$ under the condition of nonexistence of residual gas was weaker than under the condition of existence of residual gas from figure 10 and 19, chemiluminescence under the condition of nonexistence of residual gas was more uniform than under the condition of existence of residual gas. Figure 10 and 19 showed history of CV value. The CV value under the condition of nonexistence of residual gas is lower than under the condition of existence of residual gas. Therefore, chemiluminescence intensity under the condition of nonexistence of residual gas is more uniform than under the condition of existence of residual gas. Inhomogeneity of in-cylinder gas temperature and gas composition generated by residual gas is thought to fluctuate of chemiluminescence intensity. However, because these pieces of data, which are two dimensional images, are integrations of three dimensional data, depth must be taken under consideration.

## 6. Summary

In this study, the effect of residual gas on HCCI combustion is investigated from flame structure using two dimensional luminescence measurements with a 4-stroke optical accessible engine and a rapid compression machine.

(1) Under the condition of existence of residual gas, the areas in which chemiluminescence occurs and those in which it does not are clearly observed. On the other hand, under the condition of nonexistence of residual gas, the areas in which chemiluminescence does not occur are not observed.

(2) CV value is used as an index of the distribution of chemiluminescence intensity. Chemiluminescence intensity under the condition of nonexistence of residual gas is more uniform throughout the combustion chamber than under the condition of existence of residual gas.

From these results, it is presumed that inhomogeneity of temperature and composition generated by residual gas cause the distribution of the HCCI combustion flame spatial structure and chemiluminescence intensity.

## Reference

[1] M. Sjöand, J. E. Dec, N. P. Cernansky, “Potential of Thermal Stratification and Combustion Retard for Reducing Pressure-Rise Rates in HCCI Engines, Based on Multi-Zone Modeling and Experiments”, SAE Paper 2005-01-0113, (2005)

[2] K. Saijo, T. Kojima, K. Nishiwaki, Y. Yoshihara, “Numerical Prediction Method for the Combustion Process in a Homogeneous Charge Compression Ignition Engine”, JSME annual conference Vol.3, pp133-13, 2003

[3] K. Saijo, K. Nishiwaki, T. Kojima, “A Numerical Analysis of the Effect of Mixture Heterogeneity on Combustion in an HCCI Engine”, JSME annual conference Vol.3, pp77-78, 2004

[4] K. Kumano, and N. Iida, “ Analysis of the Effect of Charge Inhomogeneity on HCCI Combustion by Chemiluminescence measurement ”, SAE Paper,2004-01-1902 （2004）

[5] Y. Yamasaki, N. Iida, “Spectrum Analysis of Auto-Ignition and Combustion of Fuel / Air Pre-Mixtures”, Proceedings of the 40st Symposium (Japanese) on Combustion, pp85-86, 2002

[6] A.G.Gaydon, ”The Spectroscopy of Frames”, London Chapman and Hall, 2nd edition, pp.127-143, 282-295, 352-353, 1974